LANGMUIR

pubs.acs.org/Langmuir
Article

Surface Hydroxylation-Induced Electrostatic Forces Thicken Water Films on Quartz

Abdullah Cihan,* Piotr Zarzycki, and Zhao Hao

Cite This: *Langmuir* 2024, 40, 15099−15106
Read Online

ACCESS | Metrics & More | Article Recommendations | Supporting Information

ABSTRACT: Aqueous films on mineral surfaces control the physical, chemical, and biological transport processes in the atmosphere, soil, and rocks. Despite the importance of thin films for various research and engineering fields, there are still unanswered questions regarding the roles of the different forces affecting the nature of water films. One of these, the focus of this study, is the development of abnormally thick water films on quartz surfaces. In this study, we developed a density-functional-theory-based model to describe the time-dependent evolution of water films and identify the governing forces responsible for thickening films. We simulated the diffusion of water vapor from ambient air toward mineral surfaces and the formation and thickening of water films at various relative humidity values. Our model predicts an abnormal water film thickness on a hydroxylated quartz surface compared to a surface free of hydroxylation, which explains experimental observations. We further used the model to understand the key interaction forces at different stages of water film formation and thickening. Our model suggests that the attractive hydrogen bonding and van der Waals forces initiate a seed layer of water, and the electrostatic forces, generated by the hydroxylated and thus charged surface, lead to the thickening of water films. This generalizable model can provide insights into the peculiarities of water film development on various mineral surfaces.

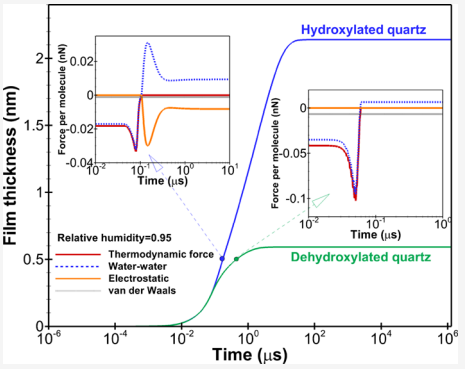

INTRODUCTION

Water film thicknesses on mineral surfaces have control over many transport processes in the atmosphere, soil, and rocks. Thin water films can limit the transport of colloids and chemicals and control the dissolution of minerals.[1−5] Therefore, quantitative understanding of the film thicknesses on mineral surfaces has been the subject of various research and engineering fields.[6−9]

Despite progress made over many decades to understand and quantify water−mineral interaction forces, how water films evolve on minerals is not completely understood.[10,9] The focus of this study is to understand some peculiarities of water films observed on quartz, the most common mineral of the earth's upper crust. Existing data from the literature imply that adsorption of water on quartz strongly depends on the hydroxylation degree, showing two distinct film thicknesses on clean and dehydroxylated quartz surfaces (Figure 1). Water films observed on clean quartz surfaces at moderate to high relative humidity (rh) values appear to be much thicker than those predicted by the Derjaguin−Landau−Verwey−Overbeek (DLVO) theory and observed in the experiments with heat-dehydroxylated quartz.[11,12] The same studies found that the film thicknesses predicted by the van der Waals (vdW) forces alone were close to the thicknesses observed on heat-dehydroxylated quartz. As a result, these previous studies suggested that heating the surface of quartz (~800−1000 °C) removed the majority of the hydroxyl group, which inhibited

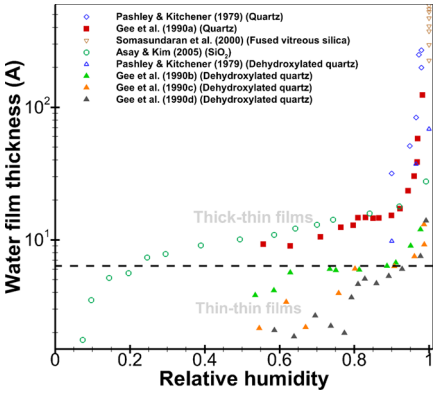

Figure 1. Water film thicknesses measured on single mineral crystals at room temperature (T = 21−25 °C). Data include significantly thick water films on clean quartz and silica surfaces compared to films on heat-dehydroxylated quartz.[11,12,14] Note that our reference to films as "thick−thin" or "thin−thin" films is only to conveniently refer to them in the text and that these are purely qualitative descriptions.

Received: April 19, 2024
Revised: June 12, 2024
Accepted: July 8, 2024
Published: July 12, 2024

https://doi.org/10.1021/acs.langmuir.4c01461
Langmuir 2024, 40, 15099−15106

ionization, hydrogen bonding, and electrostatic interactions in water adsorption on dehydroxylated quartz.[11−13] However, to the best of our knowledge, there is no theoretical study to explain the development of thick films on quartz surfaces depending on the degree of hydroxylation. A better understanding of this water−solid system requires detailed knowledge of various forces and dynamics affecting thickening of water films.

Our aim in this study is to develop and apply a theoretical model that will provide insights into the dynamics and the various interacting forces that lead to water film development under various rh conditions. We believe that the balance between water−water and water−mineral interaction forces controls the thickness of adsorbed water films on mineral surfaces. Intermolecular forces between water molecules determine the state of water in terms of density, pressure, and temperature and together with the surface tension force control the coexistence of liquid and vapor water phases. Water−solid interactions, known as surface forces, include vdW and electrostatic forces generated by charged mineral surfaces and ions present in water. In addition to these two forces that are generally included in a DLVO model, short-range hydrogen bonding (HB) and hydration forces are believed to be responsible for the structuring of water near the mineral surface,[14,15] thus playing a significant role in water film formation. Although models based on the DLVO theory have reasonably predicted the equilibrium film thickness on some mineral surfaces,[7,4] they cannot explain the dynamic nature of the transformation of adsorbed water into thick water films.

Therefore, in this study, we incorporate intermolecular, surface tension, and surface forces including the short-range hydrogen bonding into a comprehensive model based on the classical density functional theory (cDFT). Using this dynamic model, we show how water films can grow on hydroxylated quartz surfaces. Different from the previous models based on the DLVO theory and the static cDFT, our model simulates the transient diffusion of water vapor from ambient air at various rh values and the formation of liquid water on the mineral surface. The transport of water is driven by the chemical potential gradient, named the thermodynamic force that includes the contributions of water−water and water−solid interaction forces. It is known that quartz surfaces become negatively charged upon contact with adsorbed water. The charge density or electrostatic surface potential of the mineral surface, which is required as a boundary condition for the dynamic cDFT model, is deduced from a surface complexation model and literature data. The dynamic theoretical model presented below allows us to explore and identify what forces are responsible for the transformation of adsorbed water into thick water films.[16]

THEORY

In this section, we first formulate the chemical potential of water using square-gradient cDFT. Based on the chemical potential, we present model equations representing the time-dependent evolution of adsorbed water.

The Helmholtz free energy of an inhomogeneous system E_H can be expressed as

$$E_H = \int_V \psi \mathrm{d}V \tag{1}$$

where ψ is the local energy density defined as the free energy per unit volume V of a medium, expressed as

$$\psi = \psi_0 + \frac{1}{2}\kappa \nabla c \cdot \nabla c + c(\varphi_{vdW} + \varphi_{HB}) + \frac{1}{2}\rho_e \psi_e \tag{2}$$

where $\psi_0(c)$ is the homogeneous Helmholtz free energy density, defined in terms of energy per unit volume (J/m^3), and c is the molar concentration of water (mol/m^3). We employ the Fuller equation of state[17,18] to represent the homogeneous Helmholtz free energy. The second term on the right side of eq 2 represents vapor−liquid interfacial energy. The coefficient κ is known as the influence parameter (J m^5/mol^2), which is linked to the surface tension and equation of state parameters such as attraction energy and excluded volume[19,18,20] (see Supporting Information Section 1). The third term of ψ includes the vdW and the HB interaction energies between water molecules and minerals. φ_{vdW} and φ_{HB} are the interaction potentials per mole of water for the vdW and HB interactions, respectively (J/mol). φ_{vdW} for a planar water and mineral solid interface can be expressed as

$$\varphi_{vdw}(x) = \frac{-A_H}{6\pi c_{(l)}}\frac{1}{x^3} \tag{3}$$

where A_H is the Hamaker constant (J) for the interactions for the quartz−water−air system.[21,7] $c_{(l)}$ is the saturated bulk molar concentration of liquid water at a given temperature.

To represent the hydrogen bond interaction between water and mineral surface, we use an approach similar to that presented in Malheiro et al.,[22] according to which hydrogen bonding with the solid occurs only through the surface species (i.e., hydroxyl group). The number density of the species sites per area of the surface is defined as ρ_{site}. Malheiro et al.[22] assumed a constant interaction energy strength (w) within a range of the hydrogen bonding interaction (σ_{HB}). Different from Malheiro et al.,[22] here we follow Israelachvili's proposal,[23] approximating that the strength of hydrogen bonds has an inverse square-distance dependence, the same as that expected for the charge−dipole interaction: $w(r, \theta) = -Q_{H^+}u \cos\theta/(4\pi\varepsilon_0\varepsilon_{rv}r^2)$ for $r \le \sigma_{HB}$. σ_{HB} is the maximum range of the hydrogen bonding interaction that can occur between a water molecule near the surface and the available sites (hydroxyl group) at the surface. We take the magnitude of the charge Q_{H^+} and the bond moment of a hydrogen−oxygen bond u as in Israelachvili,[23] listed in Table 1. Then, by integration of the angle-averaged interactions over the mineral surface (Supporting Information Section 2), the hydrogen bonding interaction potential of a semi-infinite substrate per mole of water may be expressed as

$$\varphi_{HB}(x) = \begin{cases} -\frac{\pi\rho_{site}N_A}{3k_bT}Q^2\left(\frac{1}{x^2} - \frac{1}{\sigma_{HB}^2}\right), & x \le \sigma_{HB} \\ 0, & x > \sigma_{HB} \end{cases} \tag{4}$$

where $Q = Q_{H^+}u/(4\pi\varepsilon_0\varepsilon_{rv})$. Based on the reported values from the literature, we use ρ_{site} = 4.8 nm^{-2} for fully hydroxylated (clean) quartz and ρ_{site} = 0.4 nm^{-2} for heat-dehydroxylated quartz.

The last term in eq 2 represents the electrostatic energy density due to the presence of ions, where ρ_e is the total charge density (C/m^3) as a function of water concentration and ψ_e is the electrostatic potential (V). Silica and quartz surfaces in contact with water obtain a negative surface charge density by ionization or dissociation of silanol groups.[24,23] In this study, we focus on adsorption of water without an electrolyte solution, but "pure water" can be considered as a very dilute

https://doi.org/10.1021/acs.langmuir.4c01461
Langmuir 2024, 40, 15099−15106

Table 1. cDFT-Based Model Parameters for Water Diffusion and Adsorption (T = 20 °C)

A_H (J)	1.30×10^{-20}
ρ_{site} ($1/nm^2$)	0.4 to 4.8
σ_{HB} (nm)	0.226
Q_{H^+} (C)	0.4×10^{-19}
u (C m)	5.0×10^{-30}
$D_{(l)}$ (m^2/s)	2.02×10^{-9}
$D_{(v)}$ (m^2/s)	2.44×10^{-5}
c_{ion} ($=\chi_{ion,0} \times c_{(l)}$) ($mol/m^3$)	10^{-4}
ε_0 ($C^2/N/m^2$)	8.85×10^{-12}
$\varepsilon_{r(l)}$ (−)	80.11
$\varepsilon_{r(v)}$ (−)	1.00
v	1
F (C/mol)	96,485
k_b (J/K)	1.38×10^{-23}
R (J/K/mol)	8.314
Fuller EoS attraction energy, a ($J\ m^3/mol^2$)	9.90×10^{-1}
Fuller EoS excluded volume, b (m^3/mol)	1.55×10^{-5}
κ ($J\ m^5/mol^2$)	9.42×10^{-21}

electrolyte solution containing 10^{-7} M H_3O^+ and OH^- ions at pH = 7.[23] In multiphase liquid−vapor conditions, we use this value for the average ion concentration in liquid water and assume that the ion concentration in the air−water vapor phase is vanishingly small compared to the value in liquid water.

At equilibrium, the energy functional in eq 1 reaches a minimum, from which we derive the chemical potential of the multiphase water liquid−vapor system. The minimization of the integral (eq 1) is subject to two constraints. The first constraint is that the total moles of water (N) in the domain must be conserved: $N = \int c dV$. The second constraint is that Gauss's law, which is expressed in a differential form, must be satisfied in the system:

$$\nabla\cdot(\varepsilon\nabla\psi_e) + \rho_e = 0 \tag{5}$$

where ε is the absolute permittivity [C/(V m)] as a function of water concentration. Minimization of the functional is a problem of the calculus of variations from which the chemical potential can be formulated. Detailed mathematical derivations are presented in Supporting Information Section 3. Here, we present the result, the chemical potential as follows:

$$\Phi = \frac{\partial\psi_0}{\partial c} - \nabla\cdot\kappa\nabla c + \varphi_{vdW} + \varphi_{HB} + \frac{\partial\rho_e}{\partial c}\psi_e - \frac{1}{2}\frac{\partial\varepsilon}{\partial c}\nabla\psi_e\cdot\nabla\psi_e \tag{6}$$

where the last two terms represent the contribution of the electrostatic potential. The last term suggests that variations in the permittivity can create an additional attractive force acting on water molecules. The absolute permittivity is described as $\varepsilon = \varepsilon_0\varepsilon_r$, where ε_0 is the permittivity of the vacuum [C/(V m)] and ε_r is the dielectric coefficient or relative permittivity of water, which varies with temperature and water density. Based on the molecular dynamic simulation studies, Zarzycki[25] proposed the following approximation for the relative permittivity of water near a calcite mineral surface: $\varepsilon_r \approx \varepsilon_{r(l)}c/c_{(l)}$, where $\varepsilon_{r(l)}$ is the dielectric constant of liquid water at a given temperature, and ε_r increases with increasing concentration of water as a function time and distance. In this work, we employ a slightly modified expression, $\varepsilon_r = \varepsilon_{r(l)}c/c_{(l)} + \varepsilon_{r(v)}$, where the relative permittivity approaches the air/vacuum relative permittivity ($\varepsilon_{r(v)} \approx 1$) as c approaches the vapor concentration value for a given rh. Here, we employ an empirical relationship based on Malmberg and Maryott[26] to estimate the value of $\varepsilon_{r(l)}$ as a function of temperature.

Assuming a 1:1 monovalent-electrolyte system, the charge density can be expressed as $\rho_e = cFv\chi_{ion}$, where v is the valence, F is the Faraday constant, and χ_{ion} is the total mole fraction of positive and negative ions. Assuming the Boltzmann distribution, we can express the total mole fraction of ions as $\chi_{ion}(c, \psi_e) = \chi_{ion,0}(c)[\exp(-ev\psi_e/(k_bT)) - \exp(ev\psi_e/(k_bT))]$, where $\chi_{ion,0}$ is the ion mole fraction away from the mineral surface in the bulk, which is represented by a linear interpolation function. $\chi_{ion,0}$ is equal to the value set for the bulk liquid water, and its value approaches zero as c approaches the vapor concentration outside of the liquid zone.

Model Equations. In this work, we consider transient diffusion and adsorption of water on a mineral surface. The diffusive flux vector for water molecules, $\boldsymbol{J}$, can be expressed as

$$\boldsymbol{J} = -\frac{Dc}{RT}\nabla\Phi \tag{7}$$

when D is the effective binary diffusion coefficient of the water−air fluid system (m^2/s), T is the temperature (K), and R is the ideal gas constant (J/mol/K). Following Vignes's approach[27] used in Cihan et al.,[20,28] the effective molecular diffusion coefficient under the two-phase conditions is estimated by interpolation of the diffusivities in liquid and gas phases as $D = D_l^y \times D_g^{1-y}$, where y is $c/c_{(l)}$ and $c_{(l)}$ is the saturated bulk molar concentration of liquid water at a given T.

Substituting eq 7 for flux in water continuity, eq 8, and using it with eqs 5 and 6 together, we describe the transport of water molecules by the following three differential equations.

$$\frac{\partial c}{\partial t} + \nabla\cdot\left(-\frac{Dc}{RT}\nabla\Phi\right) = 0 \tag{8}$$

$$\Phi = \frac{\partial\psi_0}{\partial c} - \nabla\cdot\kappa\nabla c + \varphi_{vdW} + \varphi_{HB} + Fv\left(\chi_{ion} + c\frac{\partial\chi_{ion}}{\partial c}\right)\psi_e - \frac{1}{2}\frac{\partial\varepsilon}{\partial c}\nabla\psi_e\cdot\nabla\psi_e \tag{9}$$

$$\nabla\cdot(-\varepsilon_0\varepsilon_r\nabla\psi_e) = Fvc\chi_{ion} \tag{10}$$

MATERIALS AND METHODS

Experimental Data Used. We apply the model to interpret experimental observations of the adsorbed water film thicknesses on quartz surfaces at room temperature. Figure 1 presents the data obtained through multiple experimental approaches. Although no two data sets from different studies appear to be the same, they all appear to report thick−thin films on hydroxylated silica and quartz surfaces. The temperatures of the experiments by Gee et al.,[12] Asay and Kim,[14] and Somasundaran et al.[31] are reported to be around 21 °C, while the temperature of the experimental system in Pashley and Kitchener[11] is reported to be around 25 °C. From the literature, measurement of water film thickness in a controlled temperature and rh environment seems challenging. The literature appears to include two general approaches to measuring water film thicknesses, which are vapor pressure-controlled[11,12,14] and trapped or captive bubble methods.[31] Although the vapor pressure control-based methods might be more accurate for representing adsorbed water films, they may become very challenging to apply when rh approaches one because of the difficulty of accurately controlling rh near its saturation.[30,32] The differences in data sets may be attributed to differences in controlling the vapor

https://doi.org/10.1021/acs.langmuir.4c01461
Langmuir 2024, 40, 15099−15106

pressure and/or interpreting measurements from the experiments. However, Gee et al.[12] demonstrated that their vapor pressure control approach (variation of the amount of vapor admitted to the cell from a reservoir of pure water) produced water film thicknesses similar to those obtained with the approach in Pashley and Kitchener.[11] Pashley and Kitchener[11] controlled the vapor pressure by doping water with known concentrations of salts. For our model application in this study, we focus on the data presented by Gee et al.[12] because these represent water film thicknesses on both hydroxylated and dehydroxylated quartz for a wider range of rh.

Surface Complexation Model. Silica becomes charged in contact with an aqueous solution due to the protonation and deprotonation of the surface-exposed oxygen group and hydroxyls.[33] The charged surface attracts electrolyte ions, resulting in an interfacial charge distribution known as the electrical double layer. The interfacial chemistry of the silica/electrolyte interface is often described using a thermodynamic model based on the assumption that charging and ion accumulations can be described as reactions with a characteristic equilibrium constant, and spatial charge distribution can be compartmented into inner- and outer-Helmholtz layers and a diffuse part. This type of model is known as the surface complexation model (SCM), and SCMs have been developed to describe various types of mineral/electrolyte interfaces.[34−36]

In the SCM, the surface site density and surface area are intrinsically coupled parameters as they together indicate the sorption/charging capacity of a given mineral surface. Characterizing the nature and density of the surface sites experimentally is challenging. Most of the surface speciation calculations rely on the estimation of the site densities.[37] The surface area and site density are macroscopic parameters characterizing the particle suspension and thus do not reflect a single crystal face. Hydroxyl densities can be different on different surface facets of quartz. For example, X-ray spectroscopy confirms the presence of SiO^-, SiOH, and $SiOH_2^+$ sites on the silica surface but with a density much lower than expected from the crystallographic considerations.[38] According to the deuterium exchange experiments,[39] the surface site density for silica is between 5 and 11 sites/nm^2. The natural surface rarely has perfect crystal faces. Surface irregularities contribute to surface heterogeneity and reduce the amount of surface oxygen that can undergo protonation and deprotonation reactions.[37] Consequently, the lower limit of the experimentally determined site densities is often used in SCM fitting of experimental data. Here, we used the 2-p*K* triple-layer model (TLM) of the silica/electrolyte interface (see Figure S4 in the Supporting Information), similar to the model used by Li and Zarzycki.[41] We used the SCM parameter values used by Sverjensky[29] and Michael and Williams[40] to model electrokinetic and titration curves obtained for α-SiO_2. The parameters for the 2-p*K* TLM model of the silica/electrolyte solution are listed in Table S1 (Supporting Information). The SCM results (Supporting Information Figure S5) for the very low surface site density (i.e., 0.4 sites/nm^2) show a plateau in the charge density and reversal of electrostatic potential as functions of pH for pH values higher than 11. This indicates a complete saturation of the surface sites by electrolyte cations, a phenomenon that can only be observed for a very low density of the surface sites. Note that the nominal surface site density for quartz is 4.8 sites/nm^2.

Numerical Model of the Square-Gradient cDFT. To study the transient evolution of water films on a quartz surface, we use the one-dimensional version of the model presented in the Theory section. As in the experiments in Gee et al.,[12] one side of the model domain is bounded with the mineral surface, and the other side is exposed to humid air kept at fixed rh. The mineral surface is negatively charged, and we set the mineral surface potential to a constant value with respect to ambient air. A conceptual schematic description of the model boundary conditions is presented in Supporting Information Figure S6. Surface charge density corresponding to the surface potential for different surface site density values can be gleaned from the results of our surface complexation modeling presented in Supporting Information Figure S5. In this study, we do not explicitly include the Born repulsion, but no flux of water is set at the mineral surface. We employ the following initial and boundary conditions to solve the equations:

$$c(x, t = 0) = 0;\ \Phi(x, t = 0) = \Phi_0(c_v(\mathrm{rh}));\ \psi_e(x, t = 0) = 0$$
$$c(x = L, t) = c_v(\mathrm{rh});\ \Phi(x = L, t) = \Phi_0(c_v(\mathrm{rh}));$$
$$\psi_e(x = L, t) = 0,\ (\text{air - water vapor})$$
$$J(x = 0, t) = 0;\ \psi_e(x = 0, t) = \psi_{e,s},\ (\text{mineral surface}) \tag{11}$$

where L is the length of the numerical domain. For conveniently conducting the dynamical numerical solutions, we bring eqs 8−10 into the dimensionless form (Supporting Information Section 4). An in-house computer model was employed to numerically solve the coupled partial differential equations based on the finite volume method. The numerical model domain was finely discretized using a uniform dimensionless grid size of $\Delta x^* = 0.125$ (≈0.0125 nm). We chose $L \approx 100$ nm in our numerical calculations. Our sensitivity tests showed that this was large enough not to affect the predicted water film thicknesses for $0 < \mathrm{rh} \leq 0.99999$. The system of equations is linearized using the Newton−Raphson method and solved simultaneously by a preconditioned restarted generalized minimum residual algorithm. From the computed molar concentration of water, the film thickness, $h(t)$, is calculated as follows:

$$h(t) = \frac{1}{c_{(l)}} \int_0^L c(x, t)\mathrm{d}x \tag{12}$$

Table 1 lists the model input parameters used in the numerical computations for water adsorption on fully hydroxylated and dehydroxylated quartz.

Langmuir Equation and DLVO Theory-Based Model. The Langmuir equation is a simplified solution of the Poisson−Boltzmann equation which could be applicable only for very high surface electric potentials ($\psi_{e,s} \gg k_bT$) and very dilute solutions with counterions only.[42] The DLVO theory-based model includes a summation of the electrostatic (Langmuir equation) and vdW interactions of water with minerals, expressed in terms of energy per volume as $\varepsilon_0\varepsilon_{r(l)}/2[\pi k_bT/(ev)]^2/h^2 + A_H/(6\pi h^3) = -c_{(l)}RT$ ln rh. From this expression, equilibrium film thickness h is solved for different rh values. Compared with the DLVO theory-based model, our model includes the HB force with the mineral surface and is capable of predicting dynamic water thickness changes on surfaces with varying electrostatic potentials and degrees of hydroxylation.

RESULTS AND DISCUSSION

Water Film Thicknesses at Equilibrium. Before applying the dynamic cDFT model, we used an SCM, as described in the Materials and Methods section, to reveal the relationship between the degree of hydroxylation, which is represented by the surface density of mineral hydroxyl species, and the electrostatic surface potential. The SCM results are presented in the Supporting Information (Figure S5) for the surface charge density/surface potential of quartz in water as a function of pH and surface site density. The reported value of the surface potential ($\psi_{e,s} = -0.15$ V at pH = 7) for quartz in the literature[12] appears to be in reasonable agreement with the value calculated from the SCM. The surface potential value, −0.477 V, for clean quartz was reported by Israelachvili[23] for a 10^{-7} M 1:1 electrolyte representing pure water on a highly charged surface of $\sigma = -0.2$ C/m^2. Therefore, we carried out our simulation with this surface potential value for the hydroxylated quartz case. The results of the SCM (Supporting Information Figure S5) indicate that such high surface charge densities may occur for fully hydroxylated quartz at high pH. Gee et al.[12] did not measure the pH of water films; however, Mazzoco and Wayner[13] found that thick films of very dilute

https://doi.org/10.1021/acs.langmuir.4c01461
Langmuir 2024, 40, 15099−15106

electrolyte solutions stayed stable (without breaking into small droplets) only for pH > 12, which can justify the selection of the surface potential for hydroxylated quartz.

With the estimated electrostatic boundary conditions for the different degrees of hydroxylation, we applied our cDFT model to predict the adsorbed water films based on eq 16. Figure 2a shows our model predictions using the two different surface potential values, along with the experimental data from Gee et al.[12] The model successfully predicted thick water film formation at rh of higher than 0.5 on the hydroxylated quartz surface. The hydroxylation-induced large surface potentials represented in the model lead to the formation of thick water films. Meanwhile, the DLVO theory-based model appears to represent the observed data reasonably for dehydroxylated quartz where the electrostatic contributions should be less important (as demonstrated below) compared to the vdW contributions.[12] As rh approaches one, the DLVO model and the Langmuir equation predictions become closer to the data for fully hydroxylated quartz.

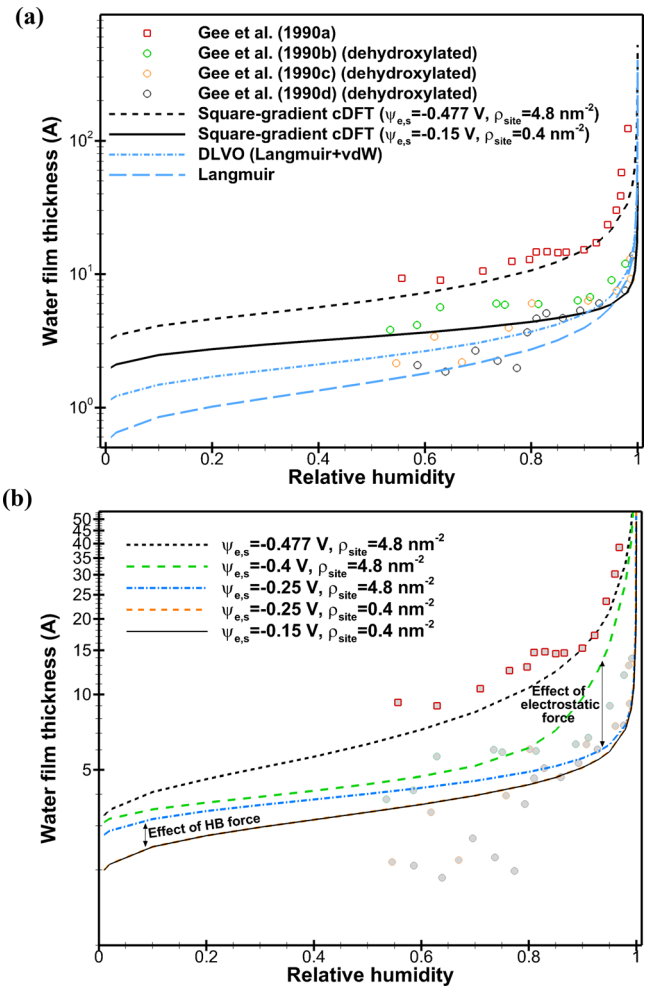

Figure 2. (a) Comparisons of the predicted adsorbed water film thicknesses at equilibrium with the measurements on quartz surfaces. (b) Sensitivity of the equilibrium film thicknesses predicted by the square-gradient cDFT model to the HB and electrostatic interactions of water with the mineral surface.

In order to illustrate how the HB and electrostatic forces contribute to the formation of the thick water films on the hydroxylated quartz surface, we calculated the thickness of water by changing the surface potential value as the model inputs. Based on the square-gradient cDFT model results, Figure 2b shows sensitivity of the equilibrium film thickness below rh = 1 to the HB and electrostatic interactions of water with the mineral surface. When $\psi_{e,s}$ = −0.15 V and ρ_{site} = 0.4 nm^{-2} (dehydroxylated quartz), the HB and electrostatic forces are much less important than the vdW forces. Changing $\psi_{e,s}$ to −0.25 V while keeping ρ_{site} constant at 0.4 nm^{-2} does not seem to affect the predicted film thicknesses, except for rh approaching one where the predicted film thickness is greater at $\psi_{e,s}$ = −0.25 V than at $\psi_{e,s}$ = −0.15 V. However, increasing ρ_{site} to 4.8 nm^{-2} while keeping $\psi_{e,s}$ = −0.25 V appears to increase the film thicknesses at lower rh values as a result of the short-range water−mineral HB interactions. The impact of the electrostatic interactions at rh values >0.5 becomes greatly pronounced when the magnitude of the surface potential is further increased (e.g., $\psi_{e,s}$ < −0.4 V) or the degree of hydroxylation approaches full hydroxylation. These results suggest that the electrostatic force mediated by surface hydroxylation is the main contributor to the growth of thick water films after initial formation on fully hydroxylated quartz. We present below a more detailed assessment of the impacts of the individual forces.

Evolution of Water Films and Forces. In order to show how individual forces contribute to the formation of thick−thin water films, we evaluated the time-dependent contribution of the forces using the numerical model results. In adsorption-driven film formation, the diffusion transports water vapor toward the mineral surface, and then subsequently water molecules are adsorbed by the action of water−mineral attractive forces. These processes are controlled by the chemical potential gradient, which we call the total thermodynamic force. The total thermodynamic force per mole of water in a one-dimensional domain is expressed by

$$f_{\mathrm{ther},x} = -\frac{\partial \Phi}{\partial x} \tag{13}$$

which contains the individual contributions of water−water and water−ion−solid interaction forces. At equilibrium ($t \to \infty$), the chemical potential gradient is equal to zero, and water−water interaction forces are balanced by water−solid and electrostatic interaction forces. The water−water interaction including intermolecular and surface tension forces per mole of water can be expressed by

$$f_{\mathrm{w-w}} = -\frac{\partial \Phi_0}{\partial x} + \kappa \frac{\partial^3 c}{\partial x^3} \tag{14}$$

The water−solid HB and vdW interaction forces are expressed, respectively, as

$$f_{\mathrm{HB},x} = -\frac{\partial \varphi_{\mathrm{HB}}}{\partial x}, \qquad f_{\mathrm{vdW},x} = -\frac{\partial \varphi_{\mathrm{vdW}}}{\partial x} \tag{15}$$

Finally, the electrostatic force per mole of water can be expressed by

$$f_{\mathrm{e},x} = -\frac{\partial}{\partial x}\left[F\nu \frac{\partial(\chi_{\mathrm{ion}} c)}{\partial c}\psi_{\mathrm{e}} - \frac{1}{2}\frac{\partial \varepsilon}{\partial c}\left(\frac{\partial \psi_{\mathrm{e}}}{\partial x}\right)^2 \right] \tag{16}$$

https://doi.org/10.1021/acs.langmuir.4c01461
Langmuir 2024, 40, 15099−15106

Figures 3 and 4 show how the individual forces change as a function of time at different distances near the mineral surface

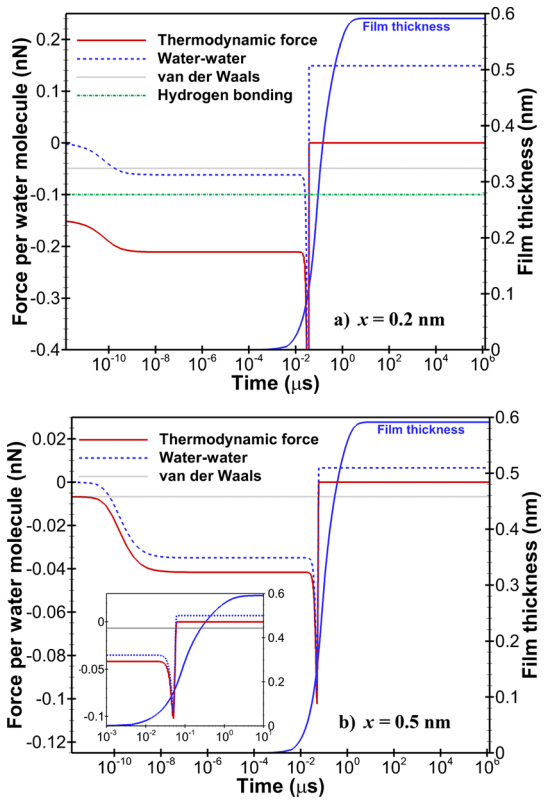

Figure 3. Time-dependent changes of forces during water film development near the dehydroxylated quartz surface (ρ_{site} = 0.4 nm^{-2}, $\psi_{e,s}$ = −0.15 V, rh = 0.95). (a) x = 0.2 nm and (b) x = 0.5 nm. The negative signs indicate force directions toward the mineral surface.

for rh = 0.95. Negative values of a force indicate that the corresponding force acts in the $-x$ direction, toward the mineral surface, and vice versa. We found that the electrostatic forces have a negligible contribution to the development of the water film on the dehydroxylated quartz surface. The films on dehydroxylated quartz seem to be formed by the water−mineral vdW and HB forces. The early time results indicate that the total thermodynamic force is directed by the actions of the attractive HB, water−water, and vdW interaction forces. This net attractive thermodynamic force causes accumulation of water molecules near the mineral surface and eventually forms a denser water phase in the vicinity of the surface (Figure 3a). When the total thermodynamic force becomes zero at equilibrium, we observe from the model results that the overall water−water interaction force is balanced by the total contributions of the attractive HB and vdW forces at very short distances ($x < \sigma_{HB}$) (Figure 3a) and by the vdW force alone at larger distances (Figure 3b). Overall, despite the lower site density (ρ_{site}), the contribution of the HB force to the short-range film formation on dehydroxylated quartz appears to be stronger than the vdW force.

As shown in Figure 4a, for water adsorption on fully hydroxylated quartz, the HB forces are much stronger at short distances from the water−mineral interface and constitute the main portion of the total thermodynamic force. At the beginning of the film formation, the water−water attractive force appears to constitute the total thermodynamic force at

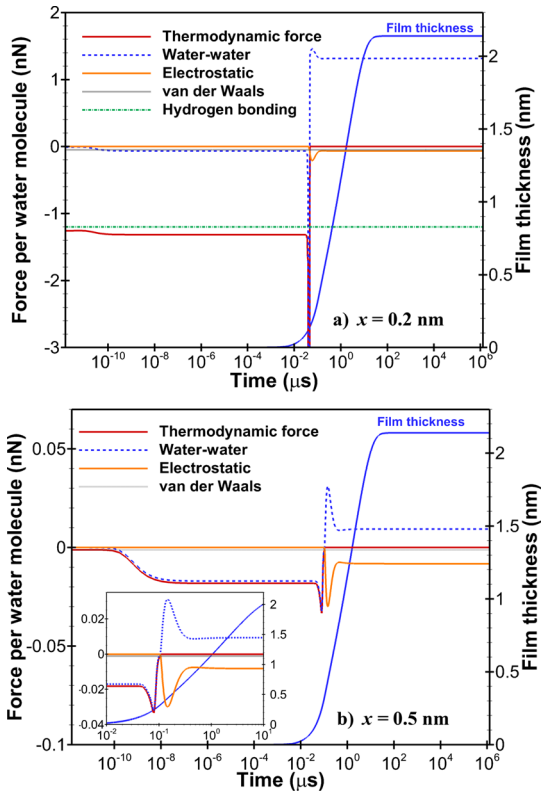

Figure 4. Time-dependent changes of forces during water film development near the hydroxylated quartz surface (ρ_{site} = 4.8 nm^{-2}, $\psi_{e,s}$ = −0.477 V, rh = 0.95). (a) x = 0.2 nm and (b) x = 0.5 nm. The negative signs indicate force directions toward the mineral surface.

larger distances, but as soon as the water film starts to form, the electrostatic force becomes a very strong attractive force because of the high surface charges. Both Figures 3 and 4 show sudden jumps in water−water interaction forces within very short time intervals during the formation of the liquid phase. The emergence of the liquid phase causes significantly high concentration gradients and activates the interfacial force near the liquid−vapor interface; this causes temporal fluctuations in the total water−water interaction forces. When the total thermodynamic force becomes zero at equilibrium, the water−water interaction force is balanced mainly by the total contributions of the attractive HB and electrostatic forces at very short distances ($x < \sigma_{HB}$) (Figure 4a) and almost solely by the electrostatic force at larger distances (Figure 4b).

Our force analyses show that water−solid attractive forces (HB and vdW) appear to form the water film in the first place, and the electrostatic forces lead to subsequent film growth and the development of thick films on highly charged quartz. The presence of higher surface charges on hydroxylated quartz surfaces increases the electrostatic potential gradient toward the surface, and hence, the chemical potential gradient increases. This enables more water molecules to be transported from ambient moist air into adsorbed liquid water compared to the transport near the dehydroxylated quartz surface. Figure 4b clearly shows that the electrostatic force becomes activated after the initial water film formation. Activation of the electrostatic force with the formation of ions in water reduces the chemical potential of the liquid water film compared to ambient moist air. The lower chemical potential of the near-surface water film enhances water vapor diffusion from moist

https://doi.org/10.1021/acs.langmuir.4c01461
Langmuir 2024, 40, 15099−15106

air and causes the film to thicken. Eventually, the chemical potentials in the liquid and vapor regions reach equilibrium and film growth stops.

Our model results show that the equilibrium film thickness is very sensitive to vapor pressure values near the saturation value and increases sharply as rh approaches unity. Although this seems generally consistent with the experimental data, the Gee et al. data for the fully hydroxylated quartz show somewhat sharper increases in water film thickness as rh approaches one. As described in the Materials and Methods section, Gee et al.[12] measured water film thicknesses using a vapor pressure-controlled method. Supporting the claim of Tokunaga,[30] our model results indicate that the very high sensitivity of film thickness requires very precise control of rh near saturation for measurement methods based on vapor pressure control. For example, our results show that the equilibrium thickness value for rh = 0.99999 is about 3.5 times greater than the equilibrium value for rh = 0.999. In addition, the time to reach the equilibrium (steady-state) thicknesses is about 10 times longer for rh = 0.99999 (Supporting Information Figure S6). It is currently unclear whether the difference between the model and data near rh = 1 is due to the limitation of the modeling approach or the uncertainty of the measurements. Moreover, the water film data of quartz for the low to moderate range of rh conditions seem to include large variations. Consequently, more precise measurement methods are needed to improve our theoretical understanding of water film formation on minerals for all rh ranges.

Our model did include a few simplifications. For example, we describe the HB force within a continuum model by averaging discrete HB interactions between the mineral surface and water molecules, and we neglected the hydration forces. The reconfiguration of the water structure near the mineral surface may lead to formation of solid-like water within the first few water layers, which is currently not included in our model prediction, although the model's equation of state allows densification of liquid water. However, implementation of a more accurate equation of state[43] may improve our prediction of condensed water phase behavior near the mineral surface. Therefore, it is unknown how this short-range structuring may affect the development of long-range thick films. Molecular dynamics or advanced DFT models can represent the local forces more accurately, but using such four-dimensional models to simulate the formation of thick water films over large spatial and temporal scales is computationally extremely challenging.

CONCLUSIONS

How thick water films are on mineral surfaces is one of the fundamental questions that deeply affect many transport processes in the atmosphere, soils, and rocks. The focus of this study is the poorly understood peculiarities of water films observed on quartz. By applying a new dynamic density-functional-theory-based model presented in this article, we provide a theoretical understanding of the development of abnormally thick water films on quartz surfaces. Our model simulates the transient diffusion of water vapor from ambient air toward mineral surfaces and the formation and thickening of water films at various rh values. We employed this model to interpret experimental data of film thicknesses on clean and dehydroxylated quartz surfaces, thus providing insights into peculiarities of water films experimentally observed on hydroxylated quartz surfaces. Our results show that the attractive HB and vdW forces initiate the formation of a thin water layer, but the electrostatic forces generated by the hydroxylated and charged surface are responsible for the thickening of water films on hydroxylated quartz surfaces. The developed modeling approach has the potential to provide insights into aqueous film development on various mineral surfaces and investigate the adsorption and transport of water in porous media.

ASSOCIATED CONTENT

Supporting Information

The Supporting Information is available free of charge at https://pubs.acs.org/doi/10.1021/acs.langmuir.4c01461.

Equation of state and surface tension of water; hydrogen bonding interaction between water and mineral surface; formulation of the chemical potential from the minimization of energy; and dimensionless model equations for adsorption and water film growth (PDF)

AUTHOR INFORMATION

Corresponding Author

Abdullah Cihan − *Energy Geosciences Division, Lawrence Berkeley National Laboratory, Berkeley, California 94720, United States;* orcid.org/0000-0002-4640-6693; Email: acihan@lbl.gov

Authors

Piotr Zarzycki − *Energy Geosciences Division, Lawrence Berkeley National Laboratory, Berkeley, California 94720, United States*

Zhao Hao − *Energy Geosciences Division, Lawrence Berkeley National Laboratory, Berkeley, California 94720, United States*

Complete contact information is available at: https://pubs.acs.org/10.1021/acs.langmuir.4c01461

Notes

The authors declare no competing financial interest.

ACKNOWLEDGMENTS

This material is based on work supported by U.S. Department of Energy (DOE), Chemical Sciences, Geosciences, and Biosciences Division under Contract DE-AC02-05CH11231.

REFERENCES

(1) Wan, J.; Tokunaga, T. K. Film straining of colloids in unsaturated porous media: Conceptual model and experimental testing. *Environ. Sci. Technol.* **1997**, *31*, 2413−2420.

(2) Tuller, M.; Or, D. Water films and scaling of soil characteristic curves at low water contents. *Water Resour. Res.* **2005**, *41*, W09403.

(3) Lebeau, M.; Konrad, J. A new capillary and thin film flow model for predicting the hydraulic conductivity of unsaturated porous media. *Water Resour. Res.* **2010**, *46*, W12554.

(4) Nishiyama, N.; Yokoyama, T. Water film thickness in unsaturated porous media: Effect of pore size, pore solution chemistry, and mineral type. *Water Resour. Res.* **2021**, *57*, No. e2020WR029257.

(5) Chen, S.; Guo, B. Pore-scale modeling of PFAS transport in water-unsaturated porous media: Air−water interfacial adsorption and mass-transfer processes in thin water films. *Water Resour. Res.* **2023**, *59*, No. e2023WR034664.

(6) Verdaguer, A.; Sacha, G. M.; Bluhm, H.; Salmeron, M. Molecular Structure of Water at Interfaces: Wetting at the Nanometer Scale. *Chem. Rev.* **2006**, *106*, 1478−1510.

(7) Tokunaga, T. K. Physicochemical controls on adsorbed water film thickness in unsaturated geological media. *Water Resour. Res.* **2011**, *47*, W08514.
(8) Björneholm, O.; et al. Water at Interfaces. *Chem. Rev.* **2016**, *116*, 7698−7726.
(9) Gonella, G.; et al. Water at charged interfaces. *Nat. Rev. Chem.* **2021**, *5*, 466−485.
(10) Ewing, G. E. Ambient Thin Film Water on Insulator Surfaces. *Chem. Rev.* **2006**, *106*, 1511−1526.
(11) Pashley, R. M.; Kitchener, J. A. Surface forces in adsorbed multilayers of water on quartz. *J. Colloid Interface Sci.* **1979**, *71*, 491.
(12) Gee, M. L.; Healy, T. W.; White, L. R. Hydrophobicity Effects in the Condensation of Water Films on Quartz. *J. Colloid Interface Sci.* **1979**, *140*, 450−465.
(13) Mazzoco, R. R.; Wayner, P. C. Aqueous Wetting Films on Fused Quartz. *J. Colloid Interface Sci.* **1999**, *214*, 156−169.
(14) Asay, D. B.; Kim, S. H. Evolution of the Adsorbed Water Layer Structure on Silicon Oxide at Room Temperature. *J. Phys. Chem. B* **2005**, *109*, 16760−16763.
(15) Chen, L.; He, X.; Liu, H.; Qian, L.; Kim, S. H. Water Adsorption on Hydrophilic and Hydrophobic Surfaces of Silicon. *J. Phys. Chem. C* **2018**, *122*, 11385−11391.
(16) Kolesnikov, A. L.; Budkov, Y. A.; Barbosa, G. D.; Mollmer, J.; Tavares, F. W. Water adsorption on planar interfaces: Classical density functional study. *Fluid Phase Equilib.* **2023**, *564*, No. 113567.
(17) Fuller, G. G. A modified Redlich-Kwong-Soave equation of state capable of representing the liquid state. *Ind. Eng. Chem. Fundam.* **1976**, *4* (15), 254−257.
(18) Guerrero, M. I.; Davis, H. T. Gradient theory of surface tension of water. *Ind. Eng. Chem. Fundam.* **1980**, *19*, 309−311.
(19) Carey, B. S.; Scriven, L. E.; Davis, H. T. Semiemprical theory of surface tensions of pure normal alkanes and alcohols. *AIChE J.* **1978**, *24* (6), 1076−1080.
(20) Cihan, A.; Tokunaga, T. K.; Birkholzer, J. T. Diffusion-to-Imbibition transition in water sorption in nanoporous media: Theoretical studies. *Water Resour. Res.* **2021**, *57*, No. e2021WR029720.
(21) French, R. H. Origins and applications of London dispersion and Hamaker constants in ceramics. *J. Am. Ceram. Soc.* **2000**, *83* (9), 2117−2146.
(22) Malheiro, C.; Mendiboure, B.; Míguez, J.-M.; Piñeiro, M. M.; Miqueu, C. Nonlocal Density Functional Theory and Grand Canonical Monte Carlo Molecular Simulations of Water Adsorption in Confined Media. *J. Phys. Chem. C* **2014**, *118* (43), 24905−24914.
(23) Israelachvili, J. N. *Intermolecular and Surface Forces*; Elsevier, 2011, 3rd ed.
(24) Behrens, S. H.; Grier, D. G. The charge of glass and silica surfaces. *J. Chem. Phys.* **2001**, *115* (14), 6716−6721.
(25) Zarzycki, P. Distance-dependent dielectric constant at the calcite/electrolyte interface: Implication for surface complexation modeling. *J. Colloid Interface Sci.* **2023**, *645*, 752−764.
(26) Malmberg, C. G.; Maryott, A. A. Dielectric constant of water from 0 to 100 C. *Journal of Research of the National Bureau of Standards* **1956**, *56* (1), 1−8.
(27) Vignes, A. Diffusion in binary solutions. *Ind. Engng J.* **1966**, *5*, 189−199.
(28) Cihan, A.; Tokunaga, T. K.; Birkholzer, J. T. Adsorption and condensation-induced imbibition in nanoporous media. *Langmuir* **2019**, *35* (29), 9611−9621.
(29) Sverjensky, D. A. Prediction of surface charge on oxides in salt solutions: Revisions for 1:1 (M+L-) electrolytes. *Geochim Cosmochim Ac* **2005**, *69* (2), 225−257.
(30) Tokunaga, T. K. Reply to Comment by Philippe Baveye on "Physicochemical controls on adsorbed water film thickness in unsaturated geological media. *Water Resour. Res.* **2012**, *48*, W11803.
(31) Somasundaran, P.; Simpson, S.; Jain, R. K.; Ivanov, I.; Raghuraman, V. Investigation of thin aqueous films on silica using a modified interferometric technique. *J. Colloid Interface Sci.* **2000**, *225* (1), 243−246.
(32) Baveye, P. C. Comment on "Physicochemical controls on adsorbed water film thickness in unsaturated geological media" by Tetsu K. Tokunaga. *Water Resour. Res.* **2012**, *48*, No. W11804.
(33) Legrand, A. P. *Silica and Related Surfaces: Interactions with Water, Encyclopedia of Surface and Colloid Science*; CRC Press, 2015, 3rd ed.
(34) Lutzenkirchen, J. *Surface Complexation Modelling*; Elsevier: Amsterdam, 2006.
(35) Lutzenkirchen, J. *Surface Complexation Models of Adsorption, Encyclopedia of Surface and Colloid Science*; CRC Press, 2015, 3rd ed.
(36) Zarzycki, P.; Charmas, R.; Piasecki, W. Formal mathematical analysis of the existence of the common intersection point in relation to determining the parameters describing ion adsorption at the oxide/electrolyte interface: Comparison of the triple and four-layer models. *Adsorption* **2004**, *10* (2), 139−149.
(37) Kosmulski, M. *Surface charging and points of zero charge*; CRC, 2009.
(38) Duval, Y.; Mielczarski, J. A.; Pokrovsky, O. S.; Mielczarski, E.; Ehrhardt, J. J. Evidence of the Existence of Three Types of Species at the Quartz−Aqueous Solution Interface at pH 0−10: XPS Surface Group Quantification and Surface Complexation Modeling. *J. Phys. Chem. B* **2002**, *106* (11), 2937−2945.
(39) Meng, X.; Letterman, R. D. Effect of component oxide interaction on the adsorption properties of mixed oxides. *Environ. Sci. Technol.* **1993**, *27* (5), 970−975.
(40) Michael, H. L.; Williams, D. J. A. Electrochemical properties of quartz. *J. Electroanal Chem. Interfacial Electrochem* **1984**, *179* (1), 131−139.
(41) Li, C.; Zarzycki, P. A computational pipeline to generate a synthetic dataset of metal ion sorption to oxides for AI/ML exploration. *Frontiers in Nuclear Engineering* **2022**, *1*, No. 977743.
(42) Langmuir, I. Repulsive forces between charged surfaces in water, and the cause of the Jones-Ray effect. *Science* **1938**, *88*, 430−432.
(43) Rehner, P.; Gross, J. Multiobjective Optimization of PCP-SAFT Parameters for Water and Alcohols Using Surface Tension Data. *Journal of Chemical & Engineering Data* **2020**, *65* (12), 5698−5707.

https://doi.org/10.1021/acs.langmuir.4c01461
Langmuir 2024, 40, 15099−15106